HHS Public Access

Author manuscript

Matrix Biol. Author manuscript; available in PMC 2017 May 01.

Published in final edited form as:

Matrix Biol. 2016 ; 52-54: 284–300. doi:10.1016/j.matbio.2016.02.003.

Phosphate induces formation of matrix vesicles during odontoblast-initiated mineralization in vitro

Sandeep C. Chaudhary[1,*], **Maria Kuzynski**[1,*], **Massimo Bottini**[2,3], **Elia Beniash**[4], **Terje Dokland**[5], **Callie G. Mobley**[1], **Manisha C. Yadav**[6], **Anne Poliard**[7], **Odile Kellerman**[8], **José Luis Millán**[6], and **Dobrawa Napierala**[1]

[1]Department of Oral and Maxillofacial Surgery, Institute of Oral Health Research, School of Dentistry, University of Alabama at Birmingham, Birmingham, Alabama, USA.

[2]Department of Experimental Medicine and Surgery, University of Rome Tor Vergata, Rome, Italy.

[3]Inflammatory and Infectious Disease Center, Sanford Burnham Prebys Medical Discovery Institute, La Jolla, California, USA.

[4]Department of Oral Biology, University of Pittsburgh School of Dental Medicine, Pittsburgh, Pennsylvania, USA.

[5]Department of Microbiology, University of Alabama at Birmingham, Birmingham, Alabama, USA.

[6]Sanford Children's Health Research Center, Sanford Burnham Prebys Medical Discovery Institute, La Jolla, California, USA.

[7]EA2496 UFR d'Odontologie, Université Paris Descartes, Montrouge, France.

[8]INSERM UMR-S 1124, Université René Descartes Paris 5, Centre Universitaire des Saints-Pères, Paris, France.

Abstract

Mineralization is a process of deposition of calcium phosphate crystals within a fibrous extracellular matrix (ECM). In mineralizing tissues, such as dentin, bone and hypertrophic cartilage, this process is initiated by a specific population of extracellular vesicles (EV), called matrix vesicles (MV). Although it has been proposed that MV are formed by shedding of the plasma membrane, the cellular and molecular mechanisms regulating formation of mineralization-competent MV are not fully elucidated. In these studies, 17IIA11, ST2, and MC3T3-E1 osteogenic cell lines were used to determine how formation of MV is regulated during initiation of the mineralization process. In addition, the molecular composition of MV secreted by 17IIA11 cells and exosomes from blood and B16-F10 melanoma cell line was compared to identify the molecular characteristics distinguishing MV from other EV. Western blot analyses demonstrated

To whom correspondence should be addressed: Dobrawa Napierala, University of Alabama at Birmingham, School of Dentistry, Department of Oral & Maxillofacial Surgery, 707 SDB, 1919 7th Avenue South, Birmingham, AL 35294-0007. Phone: (205) 975-4298, Fax: (205) 996-5109, ; Email: dobrawan@uab.edu.

*These authors equally contributed to this work.

that MV released from 17IIA11 cells are characterized by high levels of proteins engaged in calcium and phosphate regulation, but do not express the exosomal markers CD81 and HSP70. Furthermore, we uncovered that the molecular composition of MV released by 17IIA11 cells changes upon exposure to the classical inducers of osteogenic differentiation, namely ascorbic acid and phosphate. Specifically, lysosomal proteins Lamp1 and Lamp2a were only detected in MV secreted by cells stimulated with osteogenic factors. Quantitative nanoparticle tracking analyses of MV secreted by osteogenic cells determined that standard osteogenic factors stimulate MV secretion and that phosphate is the main driver of their secretion. On the molecular level, phosphate-induced MV secretion is mediated through activation of extracellular signal-regulated kinases Erk1/2 and is accompanied by re-organization of filamentous actin. In summary, we determined that mineralization-competent MV are distinct from exosomes, and we identified a new role of phosphate in the process of ECM mineralization. These data provide novel insights into the mechanisms of MV formation during initiation of the mineralization process.

Keywords

matrix vesicles; mineralization; phosphate; odontoblast; Erk1/2

Introduction

Extracellular vesicles (EV) is a broad term describing sub-micron size, spherical, membrane-enclosed particles released from cells to the extracellular milieu. EV are secreted from cells in various physiological and pathological conditions and can be detected in virtually all biological fluids (1, 2). They express cell surface receptors and carry biologically active proteins, lipids, and nucleic acids. It has been shown that EV have the capacity to modulate the function of target cells in an autocrine or paracrine manner, therefore they have been recognized as an integral component of the intercellular communication (2, 3). EV are highly heterogeneous and dynamic in nature. Their molecular composition reflects their cell-type of origin, pathophysiological cell state, biogenesis pathway, and biological function (2, 3).

Mineralization is a biological process by which crystals of calcium phosphate (hydroxyapatite, HA) are laid down within the fibrous extracellular matrix (ECM). Physiological mineralization occurs in skeletal and dental tissues (bone, terminal hypertrophic cartilage, dentin, cementum, and enamel). Mineralization can also occur ectopically (pathologic mineralization) in soft tissues, for example in the blood vessels (arterial calcification) or in joints during the late stages of osteoarthritis. The progression and extent of both physiologic and pathologic mineralization are regulated locally and systemically. Mineralization depends upon the availability of Ca^{2+} and PO_4^{3-} (P_i), concentration of mineralization inhibitors, and ECM composition (4–13).

P_i participates in the mineralization process in multiple ways. First, P_i is a structural component of the inorganic phase of the mineralized ECM, thus its local availability affects the rate of HA formation. Second, addition or removal of P_i to/from various ECM proteins regulates their function in mineralization (14, 15). Finally, it has been shown that P_i

regulates expression of multiple genes involved in osteogenic differentiation and the mineralization process (16–20). The P_i-induced signaling pathway is not well delineated and its mediators are largely unknown. However, it has been demonstrated that P_i signaling in mineralizing cells depends on the activity of P_i transporters and is mediated by Erk1/2, but not p38 or c-jun kinases (21–23). P_i-induced activation of Erk1/2 is bi-phasic with the first activation happening quickly, within 15–30 minutes of P_i treatment, and the second activation occurring approximately 6–8 hours later (23, 24).

Initiation of physiologic mineralization of cartilage, mantle dentin, and woven bone is facilitated by a specific population of EV, called matrix vesicles (MV). There is evidence suggesting that ectopic mineralization of arteries is also associated with increased secretion of EV from vascular smooth muscle cells with a presumptive role in supporting pathologic vascular mineralization (25). Electron microscopy demonstrated that mineralizing cells, such as hypertrophic chondrocytes and newly differentiated odontoblasts and osteoblasts, shed numerous sub-micron size (80 – 200 nm) vesicles from their plasma membrane (26–30). Therefore, it has been proposed that MV are formed by budding off the plasma membrane. The plasma membrane origin of MV has been further supported by comparative analyses of lipids and proteins, in which it was demonstrated that there are significant similarities in the molecular composition of MV and the plasma membrane of the cell of origin (31, 32). However, in two more recent studies, vesicles containing electron-dense material composed of calcium and phosphorus were detected in the cytoplasm of mouse calvarial osteoblasts, suggesting that intracellular processes may play a role in initial HA formation (33, 34).

MV have a discrete intravesicular environment as well as protein and lipid composition that together support the accumulation of high concentrations of P_i and Ca^{2+}, and subsequent HA formation. In particular, MV are enriched in tissue-nonspecific alkaline phosphatase (TNAP) and phosphoethanolamine/phosphocholine phosphatase (PHOSPHO1), whose catalytic activities provide P_i for HA formation, but have non-redundant functions in skeletal mineralization (4, 35–39). Proteomic analyses of vesicles produced by chondrocytes, osteoblast cell lines, and bone marrow stromal cells undergoing osteogenic differentiation consistently detect numerous proteins that are involved in the mineralization process and matrix remodeling. This agrees with the notion that the biological function of MV is to support mineralization (32, 40–43). Of note, MV are also enriched in Ca^{2+} transporters (annexins) which are commonly detected in many different types of EV (26, 38, 40, 43–47).

It is now recognized that cells utilize various cellular mechanisms to secrete EV of diverse biological functions. With the rising interest in using EV as diagnostic markers and therapeutic targets, it is critical to understand the differences between various populations of EV and the mechanisms regulating their secretion. In this study, we use cellular models of mineralization to gain mechanistic insights into the regulation of secretion of a specific group of EV with the biological function to promote mineralization. The goals of our study are to increase our understanding of how the mineralization process is initiated and to delineate characteristic features of mineralization-competent MV.

Results

Stimulation of osteogenic differentiation increases secretion of matrix vesicles in cellular models of mineralization

In studies using cellular models of mineralization, differentiation of progenitor cells and deposition of a mineralizing matrix is most commonly stimulated by treatment of cells with ascorbic acid and phosphate. Under these conditions, the calcium phosphate deposits in ECM are detected around day 21 of culture in most of the mineralizing cells. In our previous studies, we have shown that these standard osteogenic conditions induce rapid (within 6–8 days) mineralization of 17IIA11 cells, which is accompanied by production of MV (48–50). Therefore, we selected 17IIA11 cells as an in vitro model for studies of mineralization-competent MV biogenesis. First, to determine whether 17IIA11 cells are a representative in vitro model for MV formation under osteogenic conditions, we compared secretion of vesicles from 17IIA11 cells with other murine osteogenic cell lines derived from cells of different developmental origin. Preodontoblast-derived 17IIA11 cell line, bone marrow stromal cell-derived ST2 cell line, and calvarium osteoblast precursor-derived MC3T3-E1 cell line were grown to confluency. In all experiments, cells were cultured in vesicle-depleted medium to eliminate contamination of MV preparations by vesicles from FBS. Standard osteogenic conditions were used to induce mineralization. To ensure that all secreted vesicles were accounted for in these analyses, both ECM and conditioned media from tested cells were collected for vesicle isolation. Vesicles produced by unstimulated cells at the time of confluency (0h; base line) were compared with vesicles produced by cells within 24h, 48h, and 72h of culture in osteogenic conditions (Fig. 1). Nanoparticle tracking analyses (NTA) were used to quantify purified vesicles and determine their size.

NTA revealed that all compared cell lines secrete vesicles when cultured under standard growth conditions. However, the secretion of vesicles significantly increases upon addition of ascorbic acid and P_i (Fig. 1A and C). For 17IIA11 and ST2 cells, a significant increase in the number of secreted vesicles per cell is detected within the first 24h of growth under osteogenic conditions, while for MC3T3-E1 cells this occurs at 72h. During the first 24h of osteogenic differentiation, MV release is the highest in 17IIA11 cells (8 fold) as compared to 3.1 fold in ST2 cells and 1.9 fold in MC3T3-E1 cells (Fig. 1B). In conditioned medium, the number of vesicles increased robustly between 48h and 72h for all cell lines. At 24h, 280.8±68 vesicles/cell were detected in conditioned media of 17IIA11 cells, whereas 26500±6630 vesicles/cell were detected in ECM. Thus, the ECM vesicle fraction constitutes 98.9% of all vesicles released by 17IIA11 cells. The percentage of vesicles released to media was increased to 11.1% at 72h of 17IIA11 osteogenic differentiation. The increased contribution of vesicles in media at 72h was consistent for all analyzed cell lines (Fig. 1D). Thus, for all cell lines, the contribution of vesicles in medium to the total number of vesicles produced per cell increases with time. However, even after 72h of osteogenic differentiation, ECM vesicles (MV) constitute the vast majority of all EV secreted during the early stage of osteogenic differentiation (Fig. 1D).

The size of MV produced by 17IIA11, ST2, and MC3T3-E1 cells under osteogenic conditions was measured using NTA. These analyses showed that the size distribution of

MV does not change during osteogenic differentiation and does not vary between cell lines (Fig. 1E). In all compared cells lines, MV size distribution is in the same range of 50–220 nm, which is consistent with the reported size of MV produced by osteogenic cells (51).

In summary, supplementation of growth medium with standard mineralization-inducing factors (ascorbic acid and P_i) stimulates release of MV from all tested osteogenic cell lines in as early as 24 hours. Furthermore, these data show that MV secretion from 17IIA11 cells is comparable to other osteogenic cell lines. Therefore, the 17IIA11 cell line is used in subsequent experiments addressing the regulation of MV formation.

High cell density is required for induction of matrix vesicles secretion in response to mineralization-inducing factors

To determine the key factors regulating secretion of MV at the initiation of the mineralization process, we measured the concentration of vesicles formed by 17IIA11 cells and their size distribution under different culture conditions. First, we compared MV secretion from cells at different cellular confluency states, since cell-cell interactions play a role in the differentiation process (52). In standard osteogenic differentiation experiments, osteogenic factors are added at high cell density, since the cessation of proliferation is required to enter differentiation pathways. Furthermore, 17IIA11 cells cultured at high density, even without addition of ascorbic acid that stimulates collagen production, produce ECM containing collagen (Supplemental Fig. 1). Therefore, we sought to determine how cell density affects the secretion of MV. MV release was compared from untreated (control) and stimulated (ascorbic acid and P_i) 17IIA11 cells cultured at high (100% confluent) or low (70% confluent) cell densities. Results of this experiment showed no differences in the concentration of ECM-fraction MV at high or low cell density when cultured for 24h in standard growth medium (Fig. 2A). As expected, the comparison of MV concentration in ECM of cells grown at high density in standard versus osteogenic conditions shows significantly higher MV secretion under osteogenic conditions. However, there is no difference in the concentration of MV in ECM of stimulated and unstimulated cells grown at low density. Thus, osteogenic factors stimulate MV secretion from confluent cells only. At the same time, there is no difference in the size of MV secreted by cells grown under different cell densities and osteogenic conditions, with the majority of MV in the size range of 50–220 nm in all analyzed groups (Fig. 2B). In summary, high cell density is required for induction of MV secretion by osteogenic factors, but does not affect MV secretion during standard growth.

Osteogenic medium induces secretion of matrix vesicles from 17IIA11 cells

Our comparative analyses of vesicle secretion show that 17IIA11 cells respond to osteogenic stimuli by significantly increasing secretion of vesicles to ECM within 24h (Fig. 1A). As the next step, we compared the number of MV secreted per cell within 6h, 12h, 18h, and 24h of treatment with standard osteogenic medium (Fig. 3). These analyses revealed that there is no increase of MV number within the first 6h of treatment. Then, the number of MV secreted per cell rapidly and significantly increases within 6h-12h of osteogenic stimulation. Although MV continue to accumulate in ECM within the next 12h of osteogenic stimulation, the increase in the MV number per cell at 12–24h of osteogenic stimulation is

lower than the 6–12h time frame (Fig. 3). These data show that the highest increase in MV secretion by 17IIA11 cells takes place between 6h to 12h of treatment, suggesting that MV formation is an early event occurring at the onset of the osteogenic differentiation program.

Matrix vesicles are positive for proteins supporting mineralization

To determine if MV secreted by 17IIA11 cells have a role in mineralization and to compare MV with other EV of similar size (specifically exosomes), we analyzed their molecular composition by Western blot. For comparison, we used exosomes isolated from mouse plasma and exosomes produced by melanoma cells (B16-F10). Since there is no common molecular standard for various EV that can be used to confirm equal vesicular protein loading in Western blot analyses, we used silver staining of proteins separated by PAGE to confirm equal protein loading (Fig. 4A). This method also revealed a distinct protein banding pattern of each EV protein extract, suggesting substantial differences in molecular composition of EV from different sources. Interestingly, although the protein banding pattern of MV isolated from 17IIA11 cells cultured in standard growth medium is similar to MV isolated from cells stimulated with osteogenic factors, clear differences are detected with several bands unique for each group (Fig. 4A).

Western blot analyses demonstrated that two key mineralization supporting phosphatases, TNAP and PHOSPHO1, are detected only in vesicles secreted by 17IIA11 cells and not in plasma or melanoma exosomes (Fig. 4B). Interestingly, in MV from cells stimulated with osteogenic factors, three isoforms of TNAP were detected, while only two TNAP isoforms were detected in MV from unstimulated cells. Similarly, MV from stimulated cells contained an additional isoform of PHOSPHO1, while only one PHOSPHO1 isoform was detected in MV from unstimulated cells. Both PHOSPHO1 isoforms were detected in 17IIA11 cells cultured either in standard growth conditions or with osteogenic factors. MV from both stimulated and unstimulated 17IIA11 cells were highly positive for calcium channel protein annexin V. Consistent with published molecular phenotyping studies, which demonstrated that annexins are commonly detected in different types of EV (44), annexin V was also detected in exosomes from the melanoma cell line. However, unlike melanoma exosomes, MV were negative for exosomal markers HSP70 and CD81. A low but detectable amount of the early endosomal marker Rab5 was present in vesicles from 17IIA11 and melanoma cells. A distinguishing feature of MV from 17IIA11 cells stimulated with osteogenic factors, which contrasts them from MV from unstimulated cells and exosomes, is high expression of lysosomal membrane glycoproteins Lamp1 and Lamp2a. Of note, while MV from stimulated cells are highly positive for Lamp2a, in 17IIA11 cells this protein was barely detectable, which suggests that Lamp2a is distributed specifically to MV. Cytochrome C was also detected specifically in MV from stimulated 17IIA11 cells, while Grp78 was detected only in exosomes from melanoma cells. Antibodies against histone 3A detected three smaller-sized proteins, presumptive products of histone 3A proteolysis, in MV but not in exosomes. GAPDH and organelle proteins GM130 and histone 1 were not detected in MV. GAPDH was present only in EV from melanoma cells, which is consistent with previous reports showing GAPDH in exosomes (44).

In summary, comparative analyses of the molecular composition of MV from 17IIA11 cells stimulated with osteogenic factors, MV from unstimulated cells, and exosomes identified a distinct molecular signature of each EV sub-population (Fig. 4). MV from induced cells are specifically enriched in lysosomal proteins. Furthermore, MV from both unstimulated and induced 17IIA11 cells are negative for exosomal markers and positive for proteins providing Ca^{2+} and P_i. This suggests their function in supporting formation of HA, and hence mineralization.

Matrix vesicles from 17IIA11 cells are mineralization-competent

In order to determine, if MV secreted by 17IIA11 cells support formation of hydroxyapatite, we used two different approaches. First, the in vitro calcification assay was used (37, 53). MV isolated from 17IIA11 cells grown for 24h in standard growth medium, osteogenic medium or in standard growth medium supplemented with 10 mM P_i were incubated with varying concentrations of Ca^{2+} and 1mM ATP as a source of phosphate. Results of this assay demonstrated that all three groups of MV accumulated Ca^{2+} from the extravesicular environment in a dose-dependent fashion (Fig. 5A). Of note, the Ca^{2+} content in MV incubated with 1 mM Ca^{2+} was under the detection limit.

To further confirm the MV secreted by 17IIA11 cells are mineralization-competent, we used transmission electron microscopy (TEM) with electron diffraction (54, 55) and atomic force microscopy (AFM) phase analyses (56). In our previous studies we determined that mineralization of 17IIA11 cells ECM is visible around day 5 of culture under osteogenic conditions (48–50). Thus, to identify the mineral phase in MV, we compared MV isolated from ECM of 17IIA11 cells cultured either in standard growth medium or in osteogenic medium for 1 day (when there is no detectable ECM mineralization) and 8 days (when ECM mineralization reaches the plateau). TEM with selected area electron diffraction (SAED) detected no crystalline material in day 1 MV (Fig. 5B). Based on the presence of a very weak diffuse ring with d-spacing around 3Å, it is possible that some amorphous mineral was present in the MV collected from cells grown in osteogenic medium for 1 day (Fig. 5B). In contrast, crystalline material was detected by SAED in MV from both groups on day 8. However, in the sample derived from the cells grown in the standard growth medium only very few particles with very weak diffraction patterns were identified (Fig. 5B). Analysis of the diffraction patterns revealed weak reflections with d-spacings of 3.4 and 2.6Å, corresponding to (002) and (011) planes of HA reflections, respectively (54, 55). In contrast, particles producing strong reflections with d-spacings of 3.4Å corresponding to (002) planes of HA were found in the sample prepared from cells grown for 8 days in osteogenic medium (Fig. 5B).

The presence of HA in MV isolated from 17IIA11 cells grown under osteogenic conditions for 8 days was further confirmed by examining MV dropped onto a mica substrate and imaged by means of AFM, followed by qualitative evaluations of their internal composition by AFM phase analysis (56). MV AFM phase images showed the presence of internal spots with high phase angle (ϕ) values surrounded by regions with very low ϕ values (Fig. 5C). The spots at high ϕ values were interpreted to be caused by the presence of HA crystals under the MV membrane. HA crystals were surrounded by less crowded media, which made

the membrane deformable and able to damp AFM tip vibrations, which explains the large variations in ϕ values between the spots and the surrounding regions. Control MV had different topographic and phase properties compared to MV isolated from cells grown under osteogenic conditions. Control MV appeared smaller than MV isolated from cells grown under osteogenic conditions and had either a smooth surface (not shown) or a non-uniform surface with several irregularities that were a few to several Å tall (Fig. 5C). AFM phase images showed that these irregularities corresponded to spots with high phase surrounded by regions with lower phase values. However, the variation in ϕ values between the spots and the surrounding regions were much smaller for control MV than for MV isolated from cells grown under osteogenic conditions, thus suggesting that control MV were filled with mineral aggregates at an early mineralization stage, i.e. a nucleation core.

In summary, these results together with the Western blot data detecting Ca^{2+} and P_i providing proteins in MV (Fig. 4B), suggests that MV from 17IIA11 cells are competent to support mineralization.

Phosphate is the key inducer of matrix vesicle production by osteogenic cells

Ascorbic acid and phosphate (either in the organic form as β-glycerophosphate or in the inorganic form as Na-P_i buffer) are routinely used to stimulate osteogenic differentiation in vitro (24, 57). Ascorbic acid enhances the secretion of type I collagen, a major organic component of the mineralizing ECM (57), while phosphate is a structural component of the inorganic phase of the mineralizing ECM as well as a signaling molecule that regulates expression of multiple genes involved in mineralization (24, 57). Here we determined that treatment of osteogenic cells with ascorbic acid and P_i stimulates secretion of mineralization-competent MV (Figs. 1, 4 and 5). Therefore, we next compared secretion of MV by 17IIA11 cells stimulated with: i) both ascorbic acid and P_i; ii) P_i only; and iii) ascorbic acid only. As a control, MV from untreated 17IIA11 cells were also analyzed. Quantitation of MV secreted by cells within 24h was done using NTA. These comparative analyses showed that there are no significant differences in the number of MV secreted per cell from cells treated with either both osteogenic factors or P_i only. Furthermore, there is no significant difference in the number of MV secreted per cell from untreated cells and cells treated only with ascorbic acid (Fig. 6A). These results demonstrate that extracellular P_i is the major factor driving MV production from 17IIA11 cells, as ascorbic acid alone is not able to stimulate MV secretion from these cells within 24h. In all treatment conditions, the size distribution of secreted vesicles was similar (range of 50–220 nm, Fig. 6B).

We confirmed by cryo-electron microscopy imaging that the nano-particles secreted by 17IIA11 cells were indeed membrane vesicles. MV secreted by cells in all treatment conditions appeared to be translucent with a round shape and clear lipid bilayer (Fig. 6C). These analyses show that MV secreted by untreated 17IIA11 cells, cells treated either with ascorbic acid and P_i, or treated with P_i only have a similar morphology.

Erk1/2 activation is required for matrix vesicle production in response to phosphate

It has been shown that Pi-regulated gene expression in osteogenic cells is mediated through Erk1/2 (24, 58, 59). Therefore, the role of Erk1/2 activation in Pi-induced formation of

mineralization-competent MV was analyzed. First, to determine the dynamics of Erk1/2 activation in response to P_i in 17IIA11 cells, cells were treated with 2, 5, and 10 mM Na-P_i buffer, and the activation of Erk1/2 was assessed by Western blot at 15min, 30min, 45min, 1h, 2h, 4h, 6h, and 8h after addition of P_i (Fig. 7A). Comparison of the levels of phosphorylated (active) Erk1/2 to total Erk1/2 showed that Erk1/2 phosphorylation is highest at initial 15min to 1h after P_i treatment and is then reduced. We did not detect the second Erk1/2 activation within the 8h of P_i treatment of 17IIA11 cells and this activation pattern was consistent at all three P_i concentrations (Fig. 7A). Next, to address whether Erk1/2 is mediating the release of MV upon P_i treatment, we analyzed MV production when Erk1/2 signaling is inhibited. To do this, 17IIA11 cells were treated with 10mM Na-P_i for 12h with or without Erk1/2 inhibitor (U0126, 10 μM). Because we determined that the most robust MV production occurs within the initial 12h of osteogenic treatment (Fig. 3), and Erk1/2 activation is highest within the first 4h of P_i treatment, we added Erk1/2 inhibitor either together with P_i or after 4h, 6h, or 8h of P_i treatment. NTA showed that MV production was significantly disrupted by Erk1/2 inhibition at 0h, 4h, and 6h, but not when the Erk1/2 inhibitor was added 8h after P_i (Fig. 7B). A maximum decrease (65%) in the production of MV was observed when Erk1/2 inhibitor was added at the same time as P_i. These results demonstrate that MV release in response to P_i is dependent upon Erk1/2 activation.

Recent studies identified mineral-containing vesicles inside osteoblasts, which suggest that MV are formed inside cells (33, 34). Considering this, the involvement of the cytoskeleton in the trafficking of intracellular vesicles and the role of actin filaments assembly in MV secretion (60–62), we analyzed the role of the actin cytoskeleton in the release of MV in response to P_i. First, we analyzed whether P_i influences the organization of the cytoskeleton. To do this, we assessed filamentous actin (F-actin) cytoskeleton arrangement upon P_i treatment of 17IIA11 cells in a time-dependent manner (Fig. 7C). F-actin fibers were detected using fluorescent phalloidin staining. In untreated cells (0h), F-actin fibers were oriented randomly and resided close to the nucleus. P_i treatment resulted in more condensed and elongated F-actin fibers that were distributed throughout the cytoplasm. The changes in F-actin organization were apparent at 30min of P_i treatment and became more prominent at 1h, 3h, 6h, and 12h. To examine if Erk1/2 is involved in the Pi-induced cytoskeleton reorganization, we compared changes in F-actin organization following P_i treatment in the absence and presence of Erk1/2 inhibitor. The experimental design was the same as for the MV analyses (Fig. 7B), namely, 17IIA11 cells were treated with P_i for 12h, and the Erk1/2 inhibitor (U0126, 10 μM) was added either at the same time as P_i (0h) or 4h, 6h, or 8h after P_i treatment (Fig. 7D). We did not observe any changes in F-actin reorganization in cells treated with Erk1/2 inhibitor at any time points in comparison with cells treated with P_i without Erk1/2 inhibitor. This data suggests that while P_i alters the cytoskeletal organization of the cell, this is independent of Erk1/2 activation. However, Erk1/2 is an important mediator of MV secretion by P_i.

Discussion

Initiation of both physiologic and pathologic (ectopic) mineralization is supported by mineralization-competent MV secreted locally by cells with an active osteogenic program.

Here, we presented data showing that secretion of MV from osteogenic cells is induced by P_i through Erk1/2-mediated signaling. Furthermore, we determined that molecular characteristics of mineralization-competent MV distinguish this group of EV from exosomes not only by the presence of proteins specific for their biological function, but also intracellular proteins that may be indicative of the biogenesis pathway specific for mineralization-competent MV.

The constitutive and induced secretion of bioactive EV is now recognized as a common biological process of cell-cell communication (63–65). In this respect, MV are unique among other EV, as they do not transfer their bioactive cargo to other cells, but rather release it to the ECM. Our results show that the vast majority of vesicles produced by osteogenic cells during the early stage of osteogenic differentiation reside in ECM (Fig. 1), which is consistent with the biological function of MV in changing the properties of ECM and is in agreement with studies by Anderson et al. (66). However, it is not known whether the retention of MV in the ECM is a passive entrapment of vesicles in the ECM or an active process facilitated by molecular interactions between MV and ECM proteins. Although the collagenous network formed by 17IIA11 cells in our experimental conditions is not well developed (Supplemental Fig. 1), the 17IIA11 ECM composition and structure may be sufficient to retain MV. The small percentage of vesicles detected in conditioned medium may simply be MV that escaped from ECM. However, studies by Anderson et al. detected differences in protein banding pattern of PAGE-separated vesicle proteins isolated from matrix and medium fractions, suggesting different molecular composition (66). Thus, more detailed comparison of the molecular composition and the functional assays of vesicles isolated from ECM and conditioned medium of osteogenic cells is required to determine if these are the same or different populations of EV. Nonetheless, our data from quantitative analyses of vesicles in ECM and medium indicate that measuring vesicles only in medium may grossly underestimate the magnitude of MV production during osteogenic differentiation.

Out of the variety of available cell lines that undergo mineralization when stimulated with osteogenic factors, we selected three mouse cell lines of different embryonic origins to study secretion of MV. What distinguishes 17IIA11 cells from other osteogenic cell lines is that even under standard growth conditions, 17IIA11 cells express high mRNA levels of multiple genes involved in the mineralization process, including osteogenic transcription factors, ion channels, and ECM proteins (48–50). Consistent with their commitment to mineralization, 17IIA11 cells respond to stimulation with osteogenic factors with a rapid increase of MV secretion, whereas the secretion of MV from MC3T3-E1 and ST2 cells was delayed (Fig. 1). Furthermore, we showed that both stimulated and unstimulated 17IIA11 cells secrete MV expressing high levels of P_i-providing enzymes, TNAP and PHOSPHO1, and Ca^{2+} channel protein annexin V, which is in agreement with a biological function of supporting HA formation (Fig. 4B) (38, 39, 67, 68). Consistently, MV produced by 17IIA11 cells, regardless of their growth conditions, are able to accumulate Ca^{2+} from the extravesicular environment (Fig. 5A). The ability of MV to mineralize was further supported by detection of hydroxyapatite in MV isolated from cells grown in the presence of osteogenic factors for 8 days (Fig. 5B and 5C). Considering that 5 days of culture under osteogenic conditions is required to detect mineral depositions in ECM of 17IIA11 cells (48, 49), it is not unexpected

that MV isolated at day 1 do not contain crystalline material. While we do not have data on the rate of the HA crystal formation in MV from 17IIA11 cells, detection of only the amorphous mineral in MV at day 1 suggests that more than 24h under osteogenic conditions is required to form crystals. This, in turn, suggests that the lifespan of MV is longer than 24h. Thus, the quantitative analyses of MV at this time point provide reliable assessment of their number, while at the later time points, such quantitative analyses may be inaccurate as they are do not capture MV that have already ruptured from the growth of HA crystals. Although we have not analyzed formation of crystals at 48h and 72h MV, this may explain the lower number of MV from 17IIA11 cells at 48h and 72h in comparison with 24h (Fig. 1).

Interestingly, MV secreted by 17IIA11 cells stimulated with ascorbic acid and P_i express different isoforms of TNAP and PHOSPHO1 than MV secreted by cells cultured under standard growth conditions. Although the differences in function of these isoforms are unknown, these data indicate that the osteogenic extracellular environment not only stimulates the secretion of MV, but also changes their molecular composition.

The size and morphology of MV are similar to exosomes, which are currently the most studied EV sub-type. These two groups of EV share similarities on the molecular level, therefore it has been suggested that MV are membrane-anchored exosomes (47, 69). In our studies, histone 3a, which has been reported to be present in exosomes (70, 71), was also detected in MV (Fig. 4B). However, MV secreted by 17IIA11 cells are negative for CD81 and HSP70 proteins, which are considered typical exosomal markers (44).

Therefore, results of our studies do not support this concept of MV identity as exosomes, as their molecular profile is distinct from that of exosomes. Interestingly, we uncovered that MV released upon stimulation with osteogenic factors are enriched in the lysosomal markers Lamp1 and Lamp2a, yet these proteins are not detected in MV from untreated cells or exosomes (Fig. 4B). Of note, there is no difference in Lamp1 and Lamp2a protein levels in unstimulated and stimulated cells, thus osteogenic factors affect only the subcellular distribution of these proteins and not expression. Considering that the EV molecular composition reflects their biological function, this suggests that Lamp1 and Lamp2a are involved in mineralization. Such a role for Lamp1 has already been suggested by studies demonstrating that Lamp1 can localize on the cell surface and bind amelogenin, a major protein of organic dental enamel matrix (72, 73). Alternatively, the presence of these lysosomal markers in MV may be a footprint of their biogenesis pathway. This, in turn, supports the model of the intracellular formation of mineralization-competent MV. However, now, when it is known that multiple cellular mechanisms of vesicle formation exist, it is worth to consider that the biogenesis pathway of EV may be determined by extracellular stimuli or by the pathophysiological state of the cells, and not by the biological function of EV.

In these studies, we found that MV secretion from 17IIA11 cells can be induced by P_i alone (Fig. 5). Thus, we uncovered a new function of P_i in the mineralization process. Similar to P_i-induced expression of mineralization-related genes, this new P_i function is also mediated through Erk1/2. However, in comparison with transcriptional regulation, the secretion of

MV in response to P_i is faster, as it occurs within 6–12h of treatment, while changes in osteogenic gene expression have been reported after 24h (23). This suggests that induction of MV secretion in response to P_i does not require changes in transcription, or at least not in 17IIA11 cells, in which osteogenic factors are already expressed at high levels (48–50). This finding is relevant to physiologic mineralization of skeletal and dental tissues and may also provide a better understanding of the mechanisms of pathologic mineralization. For instance, elevated serum phosphate levels are the major factor contributing to vascular calcification, which is a common complication of chronic renal failure (74). In addition, it has been recently shown that, akin to physiologic mineralization, increased secretion of EV by vascular smooth muscle cells can be detected during pathologic mineralization (25).

We also detected that P_i induces changes in subcellular organization of F-actin. This was an intriguing finding, because secretion of MV has previously been shown to be dependent on reorganization of actin filaments (61, 62). Here, we have shown that similar to Erk1/2 activation, F-actin reorganization in response to P_i occurs rapidly, and the elongation of actin fibers and changes in their intracellular distribution can be detected as early as 30min after P_i treatment. However, inhibition of Erk1/2 activation had no effect on reorganization of F-actin in response to P_i. This suggests that these are two parallel events that occur in response to P_i independently to regulate MV secretion. Discovering that both MV secretion and reorganization of F-actin are regulated by P_i provides new insights into the molecular mechanisms of MV secretion.

Although these mechanisms still remain poorly deciphered, two recent studies have identified proteins critical for MV formation in odontoblasts: mouse genetic studies uncovered significantly reduced number of MV in mantle dentin and chondrocytes of *Phospho1*$^{-/-}$;*Alpl*$^{+/-}$ mice (36, 56), and our group demonstrated that the Trps1 transcription factor is required for MV secretion from 17IIA11 cells as well as for expression of *Phospho1* and *Alpl* (48). While the mechanism by which these phosphatases support secretion of MV is unknown, we speculate that PHOSPHO1, which uses phospholipids as substrates (75, 76), may affect MV secretion by affecting the fluidity of the plasma membrane. In contrast, TNAP, which is a major enzyme generating P_i and, thus, increasing P_i concentrations in the local cellular microenvironment (77), may support secretion of MV by providing P_i.

It is well recognized that EV present in bodily fluids are a mixed population of vesicles of different origins and functions, both of which are reflected in their molecular composition (44, 78). Therefore, there is a growing interest in using EV as biomarkers, as well as therapeutic targets. The former requires identification of the molecular hallmarks of specific biological functions or pathology, while the latter requires understanding the mechanisms of the formation of EV with specific biological functions or under specific pathophysiological conditions. Results of these studies provide mechanistic insights into the regulation of MV secretion in response to P_i, specifically in the context of osteogenic cells. Furthermore, we determined differences in the molecular composition of MV and exosomes that can be used to distinguish mineralization-competent vesicles from other EV.

Experimental Procedures

Cell lines and cell culture conditions

Mouse preodontoblast-derived 17IIA11 cell line was maintained in standard Dulbecco's Modified Eagle's Medium (DMEM, Gibco; Thermo Fisher Scientific, Logan, UT) with 5% FBS (Thermo Fisher Scientific, Logan, UT) and 100 units/ml penicillin and 100 μg/ml streptomycin (Cellgro, Manassas, VA) at 37°C and 8% CO_2 as described before (48–50). Mouse melanoma B16-F10 cell line (ATCC; Manassas, VA) was grown in DMEM supplemented with 10% FBS and penicillin/streptomycin at 37°C and 8% CO_2. Bone marrow stromal cell-derived ST2 cell line (generous gift from Dr. Steven Teitelbaum, Washington University, St. Louis) and calvarium osteoblast precursor-derived MC3T3-E1 cell line (ATCC; Manassas, VA) were maintained in α-MEM (Hyclone, Logan, UT) with 10% FBS, penicillin/streptomycin, and 2 mM L-glutamine. For osteogenic differentiation, cells were plated at 2×10^6 cells per 10cm dish and grown to confluency. Osteogenic differentiation was induced by supplementing the growth medium with 10 mM Na-P_i buffer (pH 7.4) and 50 μg/ml ascorbic acid (osteogenic medium). For MV analyses, cells were grown in standard medium depleted of exosomes. Exosome-depleted medium was made by centrifuging 20% FBS (diluted in DMEM or α-MEM) at 100,000 × g for 24h to remove serum-derived exosomes (79). To analyze Erk1/2 activation, cells were plated at 5×10^5 cells per well of 6-well plate. After 24h, the growth medium was replaced with low-serum (0.5% FBS) medium. Cells were serum-starved overnight, followed by treatment with 2, 5, or 10 mM Na-P_i buffer (pH 7.4).

Isolation and purification of vesicles

Vesicles from ECM and media (MV and EV, respectively) were purified using differential ultracentrifugation method as previously described (46, 48, 79). Briefly, cells were washed twice with PBS. MV were released from ECM by enzymatic digestion with 2.5 mg/ml collagenase IA (Sigma, St. Louis, MO) and 2 mM $CaCl_2$ for 2h at 37°C and 8% CO_2. The whole digestion mix containing fragmented ECM, vesicles, and cells was collected and centrifuged at 500 × g for 5 min to pellet the cells. Supernatant was transferred to separate tube and centrifuged at 2,000 × g for 10min to remove dead cells. Supernatant was again centrifuged at 10,000 × g for 30min to remove cell debris then at 100,000 × g for 70min to obtain the MV pellet. MV pellets were resuspended in PBS and centrifuged at 100,000 × g for 60min. Finally, the pellet was resuspended in 100 μl PBS and stored at −80°C until further use. For isolation of EV from conditioned medium, medium was collected from cells grown under experimental conditions and centrifuged as described above. Cells remaining on a dish were trypsinized at 37°C for 10min and combined with cell pellet collected after 1st centrifugation. Total number of cells was counted using hemocytometer (Hausser Scientific, Horsham, PA). EV from conditioned media of B16-F10 melanoma cells were collected after 48h of culture. EV from blood plasma and B16-F10 cells were purified using the ultracentrifugation method as described above.

Nanoparticle tracking analyses

Size and concentration of purified vesicles were determined by Nanoparticle Tracking Analysis (NTA) using NanoSight NS300 (Malvern Instruments Ltd, Worcestershire, UK).

Data acquisition and analysis was performed using NTA 2.3 Analytical Software. Five video files of 60 seconds at camera level 10 from each sample were recorded. Detection threshold limit 10 was used to analyze size and concentration of vesicles. Resultant concentration of MV was divided by total number of cells to calculate the production of MV per cell.

Cryo-electron microscopy

MV suspended in TBS buffer (50 mM Tris–HCl, pH 7.4 and 154 mM NaCl) were applied to holey carbon film (Quantifoil Micro Tools) and vitrified in liquid ethane using an FEI Vitrobot Mark IV. The grids were transferred to a Gatan 626 cryo-sample holder and imaged in an FEI Tecnai F20 electron microscope operated at 200 kV and nominal magnifications ranging from 32,750× to 65,500×. Low-dose images were captured with a Gatan Ultrascan 4000 CCD camera.

Transmission electron microscopy

Suspensions of MV in 70% ethanol were placed on carbon coated Ni grids and air dried. The samples were analyzed using Joel 2100 TEM (Peabody, MA) at 200 kV in bright field and selected area electron diffraction (SAED) modes. Images were acquired using Gatan CCD camera (Warrendale, PA).

Atomic force microscopy

Five microliters of MV solution was dropped onto a freshly cleaved mica substrate (Ted Pella, Redding, CA) and allowed to stand for a couple of minutes. Next, the substrate was rinsed with ddH_2O and dried at room temperature overnight. Samples were imaged by non-contact (AAC) mode in air using a 5500 AFM (Agilent Technologies). Silicon-nitride cantilevers with a nominal resonance frequency of ~190 kHz (NanosensorsTM, Neuchatel, Switzerland) were employed. Topography, amplitude and phase images were recorded for each scanned field and three-dimensional AFM images were generated by PicoView software (Agilent Technologies).

In vitro mineralization assay

MV isolated from 17IIA11 cells were assessed in vitro for their ability to mineralize as described earlier (37, 53). Briefly, 1×10^{10} MV were incubated with $CaCl_2$ (1 mM, 2mM, or 4mM) and 1 mM ATP as a phosphodiester substrate in calcifying solution (1.6 mM KH_2PO_4, 1 mM $MgCl_2$, 85 mM NaCl, 15 mM KCl, 10 mM $NaHCO_3$, 50 mM PBS, pH 7.6) at 37°C for 5.5 h. The reaction was stopped by centrifuging at 8800 × g for 30 min to pellet MV. The pellet was solubilized by adding 0.6 N HCl for 24h. The Ca^{2+} content in the MV pellet was determined by the *O*-cresolpthalein complexone method (Calcium colorimetric assay kit, Sigma-Aldrich, St. Luis, MO).

Western blot analysis

Whole protein extracts from cells and vesicles were prepared in RIPA lysis buffer supplemented with phosphatases and protease inhibitors: 1 mM NaF, 2 mM Na_2VO_4, 2 mM leupeptin, 2 mM pepstatin, 2 mM PMSF, and 10 μM MG132. Protein concentration was determined by micro BCA protein assay kit (Thermo Scientific, Rockford, IL). Protein (10

μg) was subjected to electrophoresis on 4–12% precast BisTris gels (Invitrogen) and transferred onto a nitrocellulose membrane. Specific proteins were detected by fluorescence (Li-Cor Odyssey Infrared Imaging System, LI-COR Biosciences, Lincoln, NE). Primary antibodies against tissue-nonspecific alkaline phosphatase (1:1000; R&D Systems), PHOSPHO1 (1:500; Abd Serotec), annexin V (1:2000; Abcam), α-tubulin (1:10,000; Sigma), Rab5 (1:1000; Abcam), GM130 (1:1000; Abcam), Grp78 (1:500; Santa Cruz), Gapdh (1:1000; Cell signaling), Hsp70 (1:1000; System biosciences), CD81 (1:500; Santa Cruz), Lamp1 (1:1000; Abcam), Lamp2a (1:1000; Abcam), cytochrome C (1:500; Santa Cruz), histone 1 (1:1000; Abcam), histone 3a (1:5000; Abcam), Col1a1 (1:5000; Abcam), phospho-Erk1/2 (1:2000; Cell Signaling), and Erk1/2 (1:1000; Cell Signaling) were used. All fluorescent secondary antibodies (LI-COR Biosciences; Lincoln; NE) were used at 1:20,000 dilution. Proteins separated by gel electrophoresis were visualized using Pierce Silver Stain Kit (Thermo Scientific, MA) according to manufacturer's protocol.

F-actin staining

Cells (2×10^5/well) were plated on poly-L-Lysine-coated cover slip (Fischer Scientific, MA) in 24-well plate. After 24h, cells were treated with 10 mM Na-P_i with or without 10 μM Erk1/2 inhibitor U0126 (Cell signaling, MA). For filamentous actin (F-actin) detection, cells were fixed with 4% paraformaldehyde and stained with phalloidin (1:50, Life technologies, Carlsbad, CA) for 30min at room temperature. Finally, cells were mounted with Prolong Gold antifade reagent with DAPI (Life Technologies, Carlsbad, CA). F-actin organization was imaged under Nikon A1 High Speed Confocal Laser Microscope.

Statistical analysis

All experiments were performed at least three times. Data are presented as the mean ± SD. Probability values were calculated using the Student's *t* test. $p<0.05$ (*) and <0.005 (**) were considered to be statistically significant and highly significant, respectively.

Supplementary Material

Refer to Web version on PubMed Central for supplementary material.

Acknowledgments

We thank Dr. Steven Teitelbaum (Washington University, St. Louis, MO) for providing ST2 cells and Mr. Yang Xu (University of Pittsburgh, PA) for help in the preparation of TEM samples. TEM was carried out at the Nanoscale Fabrication and Characterization Facility at Peterson Institute of Nanoscience and Engineering, University of Pittsburgh. Cryo-electron microscopy was carried out at the UAB cryo-EM core facility. We are also thankful to the UAB High Resolution Imaging Facility for assistance with the NTA and fluorescence microscopy. This work was supported by grants R01DE023083 (to D.N.), F31DE024926 (to M.K.), DE12889 and AR53102 (to J.L.M.), and R56 DE016703 (to E.B.).

References

1. Yuana Y, Sturk A, Nieuwland R. Extracellular vesicles in physiological and pathological conditions. Blood Rev. 2013; 27:31–39. [PubMed: 23261067]
2. Yanez-Mo M, Siljander PR, Andreu Z, Zavec AB, Borras FE, Buzas EI, et al. Biological properties of extracellular vesicles and their physiological functions. J Extracell Vesicles. 2015; 4:27066. [PubMed: 25979354]

3. Colombo M, Raposo G, Thery C. Biogenesis, secretion, and intercellular interactions of exosomes and other extracellular vesicles. Annu Rev Cell Dev Biol. 2014; 30:255–289. [PubMed: 25288114]
4. Addison WN, Azari F, Sorensen ES, Kaartinen MT, McKee MD. Pyrophosphate inhibits mineralization of osteoblast cultures by binding to mineral, up-regulating osteopontin, and inhibiting alkaline phosphatase activity. J Biol Chem. 2007; 282:15872–15883. [PubMed: 17383965]
5. Giachelli CM, Speer MY, Li X, Rajachar RM, Yang H. Regulation of vascular calcification: roles of phosphate and osteopontin. Circ Res. 2005; 96:717–722. [PubMed: 15831823]
6. Johnson K, Goding J, Van Etten D, Sali A, Hu SI, Farley D, et al. Linked deficiencies in extracellular PP(i) and osteopontin mediate pathologic calcification associated with defective PC-1 and ANK expression. J Bone Miner Res. 2003; 18:994–1004. [PubMed: 12817751]
7. Lomashvili KA, Narisawa S, Millan JL, O'Neill WC. Vascular calcification is dependent on plasma levels of pyrophosphate. Kidney Int. 2014; 85:1351–1356. [PubMed: 24717293]
8. Luo G, Ducy P, McKee MD, Pinero GJ, Loyer E, Behringer RR, et al. Spontaneous calcification of arteries and cartilage in mice lacking matrix GLA protein. Nature. 1997; 386:78–81. [PubMed: 9052783]
9. Prosdocimo DA, Wyler SC, Romani AM, O'Neill WC, Dubyak GR. Regulation of vascular smooth muscle cell calcification by extracellular pyrophosphate homeostasis: synergistic modulation by cyclic AMP and hyperphosphatemia. Am J Physiol Cell Physiol. 2010; 298:C702–C713. [PubMed: 20018951]
10. Sallam T, Cheng H, Demer LL, Tintut Y. Regulatory circuits controlling vascular cell calcification. Cell Mol Life Sci. 2013; 70:3187–3197. [PubMed: 23269436]
11. Schurgers LJ, Cranenburg EC, Vermeer C. Matrix Gla-protein: the calcification inhibitor in need of vitamin K. Thromb Haemost. 2008; 100:593–603. [PubMed: 18841280]
12. Szeberin Z, Fehervari M, Krepuska M, Apor A, Rimely E, Sarkadi H, et al. Serum fetuin-A levels inversely correlate with the severity of arterial calcification in patients with chronic lower extremity atherosclerosis without renal disease. Int Angiol. 2011; 30:474–450. [PubMed: 21804488]
13. Westenfeld R, Jahnen-Dechent W, Ketteler M. Vascular calcification and fetuin-A deficiency in chronic kidney disease. Trends Cardiovasc Med. 2007; 17:124–128. [PubMed: 17482094]
14. Sodek J, Ganss B, McKee MD. Osteopontin. Crit Rev Oral Biol Med. 2000; 11:279–303. [PubMed: 11021631]
15. McKnight DA, Fisher LW. Molecular evolution of dentin phosphoprotein among toothed and toothless animals. BMC Evol Biol. 2009; 9:299. [PubMed: 20030824]
16. Foster BL, Nociti FH Jr, Swanson EC, Matsa-Dunn D, Berry JE, Cupp CJ, et al. Regulation of cementoblast gene expression by inorganic phosphate in vitro. Calcif Tissue Int. 2006; 78:103–112. [PubMed: 16467974]
17. Khoshniat S, Bourgine A, Julien M, Weiss P, Guicheux J, Beck L. The emergence of phosphate as a specific signaling molecule in bone and other cell types in mammals. Cell Mol Life Sci. 2011; 68:205–218. [PubMed: 20848155]
18. Kumar R. Phosphate sensing. Curr Opin Nephrol Hypertens. 2009; 18:281–284. [PubMed: 19352177]
19. Julien M, Magne D, Masson M, Rolli-Derkinderen M, Chassande O, Cario-Toumaniantz C, et al. Phosphate stimulates matrix Gla protein expression in chondrocytes through the extracellular signal regulated kinase signaling pathway. Endocrinology. 2007; 148:530–537. [PubMed: 17068135]
20. Julien M, Khoshniat S, Lacreusette A, Gatius M, Bozec A, Wagner EF, et al. Phosphate-dependent regulation of MGP in osteoblasts: role of ERK1/2 and Fra-1. J Bone Miner Res. 2009; 24:1856–1868. [PubMed: 19419315]
21. Razzaque MS. Phosphate and Vitamin D in Chronic Kidney Disease. Contributions to Nephrology. 2013; 180:74–85. [PubMed: 23652551]
22. von Kriegsheim A, Baiocchi D, Birtwistle M, Sumpton D, Bienvenut W, Morrice N, et al. Cell fate decisions are specified by the dynamic ERK interactome. Nat Cell Biol. 2009; 11:1458–1464. [PubMed: 19935650]

23. Camalier CE, Yi M, Yu LR, Hood BL, Conrads KA, Lee YJ, et al. An integrated understanding of the physiological response to elevated extracellular phosphate. J Cell Physiol. 2013; 228:1536–1550. [PubMed: 23280476]
24. Tada H, Nemoto E, Foster BL, Somerman MJ, Shimauchi H. Phosphate increases bone morphogenetic protein-2 expression through cAMP-dependent protein kinase and ERK1/2 pathways in human dental pulp cells. Bone. 2011; 48:1409–1416. [PubMed: 21419244]
25. Kapustin AN, Chatrou ML, Drozdov I, Zheng Y, Davidson SM, Soong D, et al. Vascular smooth muscle cell calcification is mediated by regulated exosome secretion. Circ Res. 2015; 116:1312–1323. [PubMed: 25711438]
26. Anderson HC, Harmey D, Camacho NP, Garimella R, Sipe JB, Tague S, et al. Sustained osteomalacia of long bones despite major improvement in other hypophosphatasia-related mineral deficits in tissue nonspecific alkaline phosphatase/nucleotide pyrophosphatase phosphodiesterase 1 double-deficient mice. Am J Pathol. 2005; 166:1711–17120. [PubMed: 15920156]
27. Garces-Ortiz M, Ledesma-Montes C, Reyes-Gasga J. Presence of matrix vesicles in the body of odontoblasts and in the inner third of dentinal tissue: a scanning electron microscopic study. Med Oral Patol Oral Cir Bucal. 2013; 18:e537–e541. [PubMed: 23385510]
28. Katchburian E. Membrane-bound bodies as initiators of mineralization of dentine. J Anat. 1973; 116:285–302. [PubMed: 4783420]
29. Magne D, Bluteau G, Faucheux C, Palmer G, Vignes-Colombeix C, Pilet P, et al. Phosphate is a specific signal for ATDC5 chondrocyte maturation and apoptosis-associated mineralization: possible implication of apoptosis in the regulation of endochondral ossification. J Bone Miner Res. 2003; 18:1430–1442. [PubMed: 12929932]
30. Rilla K, Pasonen-Seppanen S, Deen AJ, Koistinen VV, Wojciechowski S, Oikari S, et al. Hyaluronan production enhances shedding of plasma membrane-derived microvesicles. Exp Cell Res. 2013; 319:2006–2018. [PubMed: 23732660]
31. Abdallah D, Hamade E, Merhi RA, Bassam B, Buchet R, Mebarek S. Fatty acid composition in matrix vesicles and in microvilli from femurs of chicken embryos revealed selective recruitment of fatty acids. Biochem Biophys Res Commun. 2014; 446:1161–1164. [PubMed: 24685481]
32. Balcerzak M, Malinowska A, Thouverey C, Sekrecka A, Dadlez M, Buchet R, et al. Proteome analysis of matrix vesicles isolated from femurs of chicken embryo. Proteomics. 2008; 8:192–205. [PubMed: 18095356]
33. Boonrungsiman S, Gentleman E, Carzaniga R, Evans ND, McComb DW, Porter AE, et al. The role of intracellular calcium phosphate in osteoblast-mediated bone apatite formation. Proc Natl Acad Sci U S A. 2012; 109:14170–14175. [PubMed: 22879397]
34. Mahamid J, Sharir A, Gur D, Zelzer E, Addadi L, Weiner S. Bone mineralization proceeds through intracellular calcium phosphate loaded vesicles: a cryo-electron microscopy study. J Struct Biol. 2011; 174:527–535. [PubMed: 21440636]
35. Barron MJ, McDonnell ST, Mackie I, Dixon MJ. Hereditary dentine disorders: dentinogenesis imperfecta and dentine dysplasia. Orphanet J Rare Dis. 2008; 3:31. [PubMed: 19021896]
36. McKee MD, Yadav MC, Foster BL, Somerman MJ, Farquharson C, Millan JL. Compounded PHOSPHO1/ALPL deficiencies reduce dentin mineralization. J Dent Res. 2013; 92:721–727. [PubMed: 23694930]
37. Roberts S, Narisawa S, Harmey D, Millan JL, Farquharson C. Functional involvement of PHOSPHO1 in matrix vesicle-mediated skeletal mineralization. J Bone Miner Res. 2007; 22:617–627. [PubMed: 17227223]
38. Yadav MC, Simao AM, Narisawa S, Huesa C, McKee MD, Farquharson C, et al. Loss of skeletal mineralization by the simultaneous ablation of PHOSPHO1 and alkaline phosphatase function: a unified model of the mechanisms of initiation of skeletal calcification. J Bone Miner Res. 2011; 26:286–297. [PubMed: 20684022]
39. Huesa C, Houston D, Kiffer-Moreira T, Yadav MM, Millan JL, Farquharson C. The Functional co-operativity of Tissue-Nonspecific Alkaline Phosphatase (TNAP) and PHOSPHO1 during initiation of Skeletal Mineralization. Biochem Biophys Rep. 2015; 4:196–201. [PubMed: 26457330]

40. Kim HS, Choi DY, Yun SJ, Choi SM, Kang JW, Jung JW, et al. Proteomic analysis of microvesicles derived from human mesenchymal stem cells. J Proteome Res. 2012; 11:839–849. [PubMed: 22148876]
41. Morhayim J, van de Peppel J, Demmers JA, Kocer G, Nigg AL, van Driel M, et al. Proteomic signatures of extracellular vesicles secreted by nonmineralizing and mineralizing human osteoblasts and stimulation of tumor cell growth. FASEB J. 2015; 29:274–285. [PubMed: 25359493]
42. Thouverey C, Malinowska A, Balcerzak M, Strzelecka-Kiliszek A, Buchet R, Dadlez M, et al. Proteomic characterization of biogenesis and functions of matrix vesicles released from mineralizing human osteoblast-like cells. J Proteomics. 2011; 74:1123–1134. [PubMed: 21515422]
43. Xiao Z, Camalier CE, Nagashima K, Chan KC, Lucas DA, de la Cruz MJ, et al. Analysis of the extracellular matrix vesicle proteome in mineralizing osteoblasts. J Cell Physiol. 2007; 210:325–335. [PubMed: 17096383]
44. Lotvall J, Hill AF, Hochberg F, Buzas EI, Di Vizio D, Gardiner C, et al. Minimal experimental requirements for definition of extracellular vesicles and their functions: a position statement from the International Society for Extracellular Vesicles. J Extracell Vesicles. 2014; 3:26913. [PubMed: 25536934]
45. Golub EE. Biomineralization and matrix vesicles in biology and pathology. Semin Immunopathol. 2011; 33:409–417. [PubMed: 21140263]
46. Kirsch T, Nah HD, Shapiro IM, Pacifici M. Regulated production of mineralization-competent matrix vesicles in hypertrophic chondrocytes. J Cell Biol. 1997; 137:1149–1160. [PubMed: 9166414]
47. Shapiro IM, Landis WJ, Risbud MV. Matrix vesicles: Are they anchored exosomes? Bone. 2015; 79:29–36. [PubMed: 25980744]
48. Kuzynski M, Goss M, Bottini M, Yadav MC, Mobley C, Winters T, et al. Dual role of the Trps1 transcription factor in dentin mineralization. J Biol Chem. 2014; 289:27481–27493. [PubMed: 25128529]
49. Lacerda-Pinheiro S, Dimitrova-Nakov S, Harichane Y, Souyri M, Petit-Cocault L, Legres L, et al. Concomitant multipotent and unipotent dental pulp progenitors and their respective contribution to mineralised tissue formation. Eur Cell Mater. 2012; 23:371–386. [PubMed: 22623164]
50. Priam F, Ronco V, Locker M, Bourd K, Bonnefoix M, Duchene T, et al. New cellular models for tracking the odontoblast phenotype. Arch Oral Biol. 2005; 50:271–277. [PubMed: 15721161]
51. Anderson HC. Vesicles associated with calcification in the matrix of epiphyseal cartilage. J Cell Biol. 1969; 41:59–72. [PubMed: 5775794]
52. Bitar M, Brown RA, Salih V, Kidane AG, Knowles JC, Nazhat SN. Effect of cell density on osteoblastic differentiation and matrix degradation of biomimetic dense collagen scaffolds. Biomacromolecules. 2008; 9:129–135. [PubMed: 18095652]
53. Garimella R, Bi X, Camacho N, Sipe JB, Anderson HC. Primary culture of rat growth plate chondrocytes: an in vitro model of growth plate histotype, matrix vesicle biogenesis and mineralization. Bone. 2004; 34:961–970. [PubMed: 15193542]
54. Cuisinier F, Bres EF, Hemmerle J, Voegel JC, Frank RM. Transmission electron microscopy of lattice planes in human alveolar bone apatite crystals. Calcif Tissue Int. 1987; 40:332–338. [PubMed: 3038280]
55. Suvorova EI, Buffat PA. Electron diffraction from micro- and nanoparticles of hydroxyapatite. J Microsc. 1999; 196:46–58. [PubMed: 10540256]
56. Yadav MC, Bottini M, Cory E, Bhattacharya K, Kuss P, Narisawa S, et al. Skeletal Mineralization Deficits and Impaired Biogenesis and Function of Chondrocyte-Derived Matrix Vesicles in Phospho1 and Phospho1/Pit1 Double Knockout Mice. J Bone Miner Res. 2016
57. Langenbach F, Handschel J. Effects of dexamethasone, ascorbic acid and beta-glycerophosphate on the osteogenic differentiation of stem cells in vitro. Stem Cell Res Ther. 2013; 4:117. [PubMed: 24073831]

58. Matsushita T, Chan YY, Kawanami A, Balmes G, Landreth GE, Murakami S. Extracellular signal-regulated kinase 1 (ERK1) and ERK2 play essential roles in osteoblast differentiation and in supporting osteoclastogenesis. Mol Cell Biol. 2009; 29:5843–5857. [PubMed: 19737917]
59. Kang JH, Toita R, Asai D, Yamaoka T, Murata M. Reduction of inorganic phosphate-induced human smooth muscle cells calcification by inhibition of protein kinase A and p38 mitogen-activated protein kinase. Heart Vessels. 2014; 29:718–722. [PubMed: 24141990]
60. Cai H, Reinisch K, Ferro-Novick S. Coats, tethers, Rabs, and SNAREs work together to mediate the intracellular destination of a transport vesicle. Dev Cell. 2007; 12:671–682. [PubMed: 17488620]
61. Hale JE, Wuthier RE. The mechanism of matrix vesicle formation. Studies on the composition of chondrocyte microvilli and on the effects of microfilament-perturbing agents on cellular vesiculation. J Biol Chem. 1987; 262:1916–1925. [PubMed: 3543016]
62. Thouverey C, Strzelecka-Kiliszek A, Balcerzak M, Buchet R, Pikula S. Matrix vesicles originate from apical membrane microvilli of mineralizing osteoblast-like Saos-2 cells. J Cell Biochem. 2009; 106:127–138. [PubMed: 19009559]
63. Kalra H, Simpson RJ, Ji H, Aikawa E, Altevogt P, Askenase P, et al. Vesiclepedia: a compendium for extracellular vesicles with continuous community annotation. PLoS Biol. 2012; 10:e1001450. [PubMed: 23271954]
64. Thery C. Exosomes: secreted vesicles and intercellular communications. F1000 Biol Rep. 2011; 3:15. [PubMed: 21876726]
65. Simons M, Raposo G. Exosomes--vesicular carriers for intercellular communication. Curr Opin Cell Biol. 2009; 21:575–581. [PubMed: 19442504]
66. Anderson HC, Stechschulte DJ Jr, Collins DE, Jacobs DH, Morris DC, Hsu HH, et al. Matrix vesicle biogenesis in vitro by rachitic and normal rat chondrocytes. Am J Pathol. 1990; 136:391–398. [PubMed: 2305834]
67. Kirsch T, Harrison G, Golub EE, Nah HD. The roles of annexins and types II and X collagen in matrix vesicle-mediated mineralization of growth plate cartilage. J Biol Chem. 2000; 275:35577–35583. [PubMed: 10956650]
68. Ciancaglini P, Yadav MC, Simao AM, Narisawa S, Pizauro JM, Farquharson C, et al. Kinetic analysis of substrate utilization by native and TNAP-, NPP1-, or PHOSPHO1-deficient matrix vesicles. J Bone Miner Res. 2010; 25:716–723. [PubMed: 19874193]
69. Rosenthal AK, Gohr CM, Ninomiya J, Wakim BT. Proteomic analysis of articular cartilage vesicles from normal and osteoarthritic cartilage. Arthritis Rheum. 2011; 63:401–411. [PubMed: 21279997]
70. Nangami G, Koumangoye R, Shawn Goodwin J, Sakwe AM, Marshall D, Higginbotham J, et al. Fetuin-A associates with histones intracellularly and shuttles them to exosomes to promote focal adhesion assembly resulting in rapid adhesion and spreading in breast carcinoma cells. Exp Cell Res. 2014; 328:388–400. [PubMed: 25194507]
71. Muthukrishnan U, Natarajan B, Rome S, Johansson HJ, Nordin JZ, Wiklander O, et al. Stress-induced changes in exosomal histone secretion in The Fourth International Meeting of ISEV, ISEV2015. J Extracell Vesicles. 2015; 4:27783. [PubMed: 25967741]
72. Tompkins K, George A, Veis A. Characterization of a mouse amelogenin [A-4]/M59 cell surface receptor. Bone. 2006; 38:172–180. [PubMed: 16214432]
73. Zhang H, Tompkins K, Garrigues J, Snead ML, Gibson CW, Somerman MJ. Full length amelogenin binds to cell surface LAMP-1 on tooth root/periodontium associated cells. Arch Oral Biol. 2010; 55:417–425. [PubMed: 20382373]
74. London GM, Guerin AP, Marchais SJ, Metivier F, Pannier B, Adda H. Arterial media calcification in end-stage renal disease: impact on all-cause and cardiovascular mortality. Nephrol Dial Transplant. 2003; 18:1731–1740. [PubMed: 12937218]
75. Roberts SJ, Stewart AJ, Sadler PJ, Farquharson C. Human PHOSPHO1 exhibits high specific phosphoethanolamine and phosphocholine phosphatase activities. Biochem J. 2004; 382:59–65. [PubMed: 15175005]

76. Roberts SJ, Stewart AJ, Schmid R, Blindauer CA, Bond SR, Sadler PJ, et al. Probing the substrate specificities of human PHOSPHO1 and PHOSPHO2. Biochim Biophys Acta. 2005; 1752:73–82. [PubMed: 16054448]

77. Millan JL. The role of phosphatases in the initiation of skeletal mineralization. Calcif Tissue Int. 2013; 93:299–306. [PubMed: 23183786]

78. Bobrie A, Colombo M, Krumeich S, Raposo G, Thery C. Diverse subpopulations of vesicles secreted by different intracellular mechanisms are present in exosome preparations obtained by differential ultracentrifugation. J Extracell Vesicles. 2012; 1:18397.

79. Thery C, Amigorena S, Raposo G, Clayton A. Isolation and characterization of exosomes from cell culture supernatants and biological fluids. Curr Protoc Cell Biol. 2006 Chapter 3:Unit 3.22.1-9.

Highlights

- Novel function of phosphate in mineralization was identified.
- Phosphate induces secretion of matrix vesicles.
- Molecular characteristics of matrix vesicles distinguish them from exosomes.

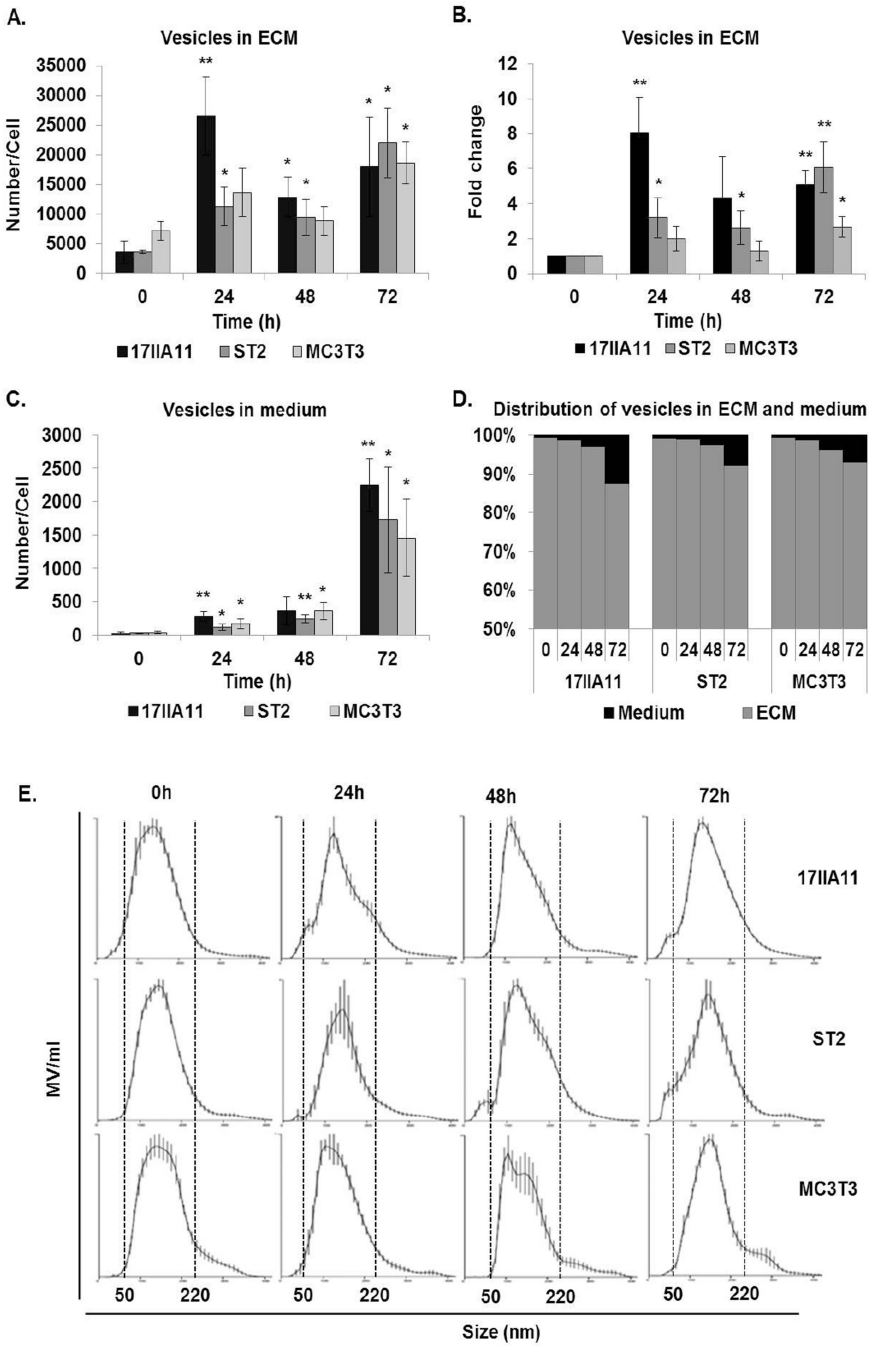

Figure 1. Osteogenic medium stimulates secretion of EV from mineralizing cell lines

The number of vesicles (A–D) and size distribution (E) were measured using nanoparticle tracking analysis. Secretion of vesicles was stimulated by standard osteogenic conditions (ascorbic acid and P_i) for 24h, 48h, or 72h and compared to unstimulated cells (0h). Vesicles were collected from the media or extracellular matrix (ECM). (A) Number of vesicles in ECM normalized to the number of cells. Statistical analyzes were performed to assess differences between mean values of unstimulated cells and the same cells at different time points of osteogenic treatment. (B) Fold changes in the number of vesicles in ECM

compared to 0h of each cell line. (C) Number of vesicles secreted to medium normalized to the number of cells. (D) Distribution of vesicles between ECM and medium. (E) Size distribution of vesicles in ECM. Dotted lines indicate the size range of vesicles for each cell line. Data are represented as the mean values of three independent experiments ± SD, *$p<0.05$ and **$p<0.005$.

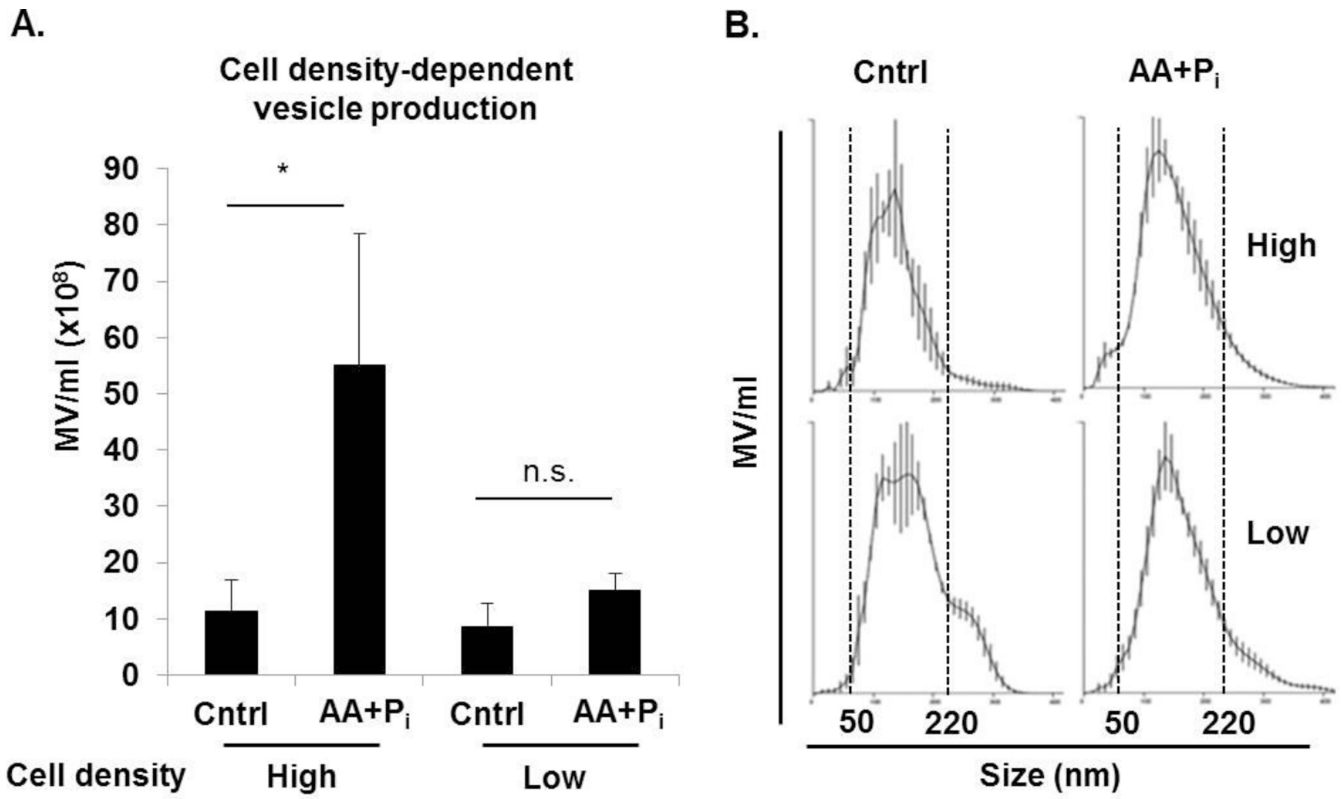

Figure 2. MV secretion upon induction of osteogenic differentiation depends on cell density

100% confluent (high) and 70% confluent (low) 17IIA11 cells were treated with standard osteogenic conditions (ascorbic acid and P_i) to stimulate vesicle secretion. Control high and low density cells were grown without osteogenic supplements. After 24h, vesicles were isolated and the number and size distribution were measured using nanoparticle tracking analysis. (A) Concentration of MV isolated from ECM of 100% confluent (high) and 70% confluent (low) cells treated with ascorbic acid and P_i, and cells cultured in standard growth medium. (B) Graphs showing MV size distribution in all culture conditions. Dotted lines indicate the size range of vesicles for each cell line. Data are represented as the mean values of three independent experiments ± SD, *$p<0.05$ and **$p<0.005$.

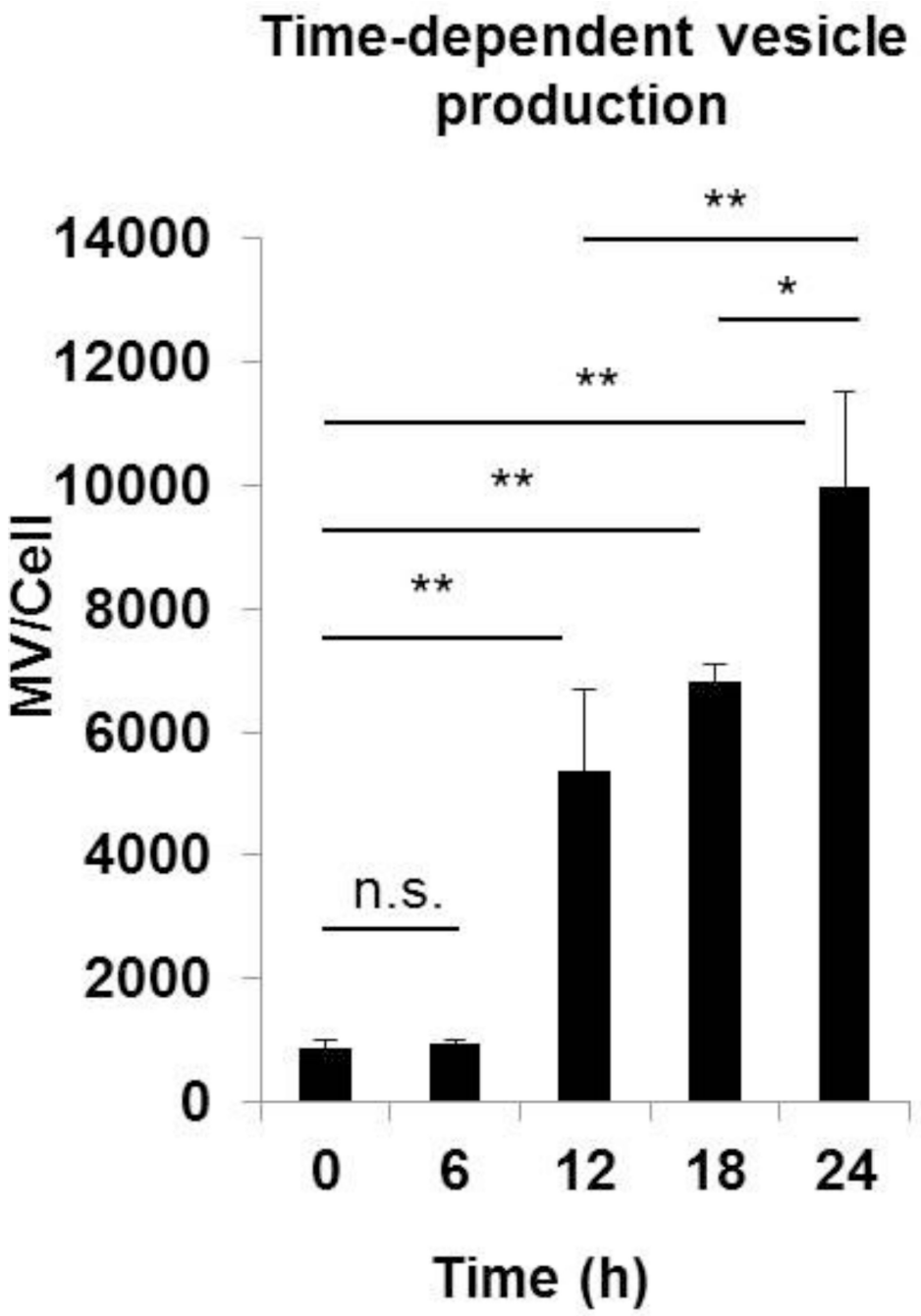

Figure 3. Osteogenic medium induces rapid secretion of MV from 17IIA11 cells

Comparison of MV concentration in ECM of 17IIA11 cells grown in standard growth conditions (0h, baseline) and in osteogenic conditions (ascorbic acid and P_i; AA + P_i) for 6h, 12h, 18h, and 24h. The number of MV secreted per cell was determined using nanoparticle tracking analysis. Data are represented as the mean values of three independent experiments ± SD, *$p<0.05$ and **$p<0.005$.

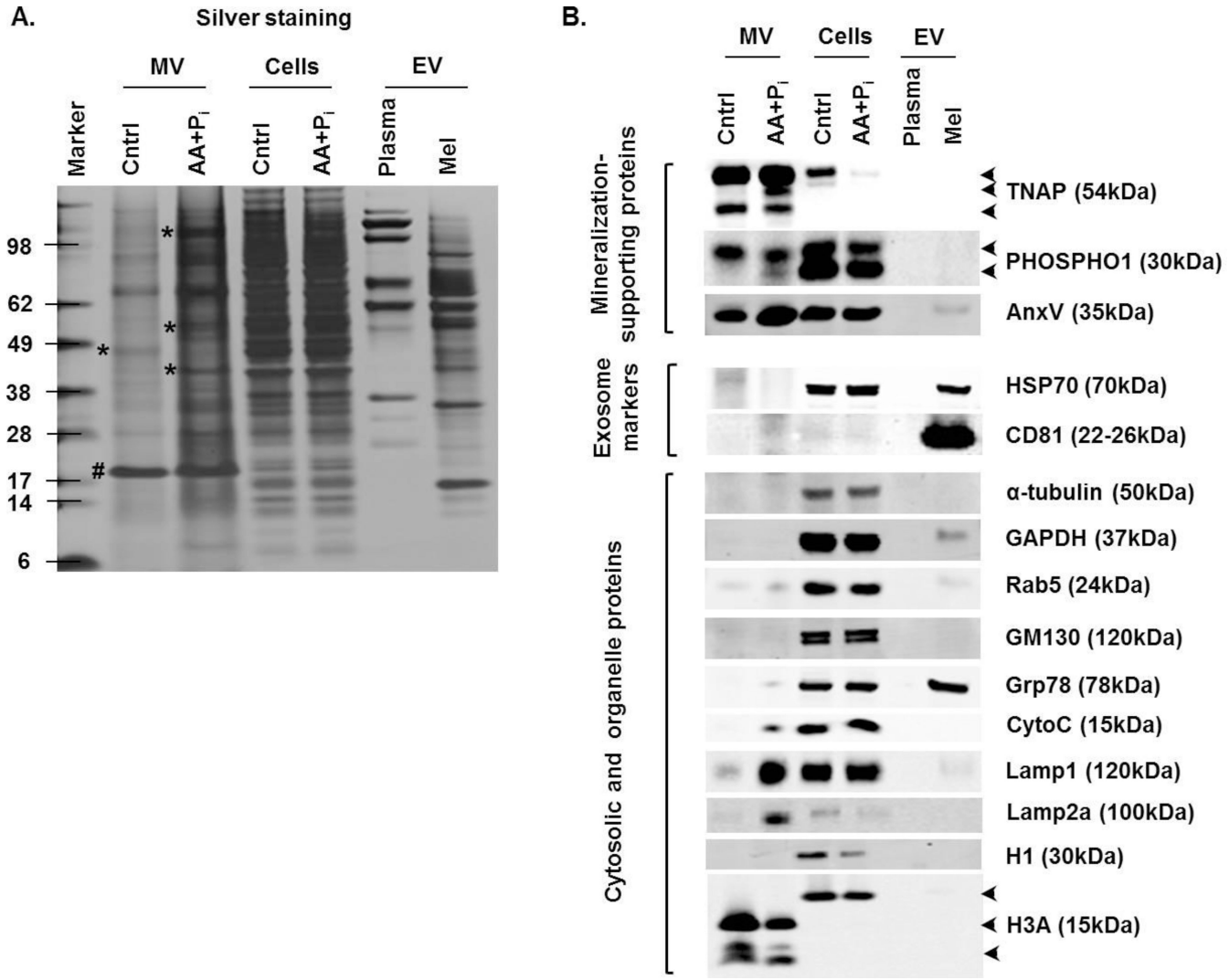

Figure 4. Osteogenic medium induces formation of mineralization-competent MV

17IIA11 cells were treated with standard osteogenic conditions (ascorbic acid and P_i; AA + P_i). Proteins from MV and 17IIA11 cells were isolated after 24h of ascorbic acid and P_i treatment. Proteins from MV and 17IIA11 cells cultured in standard growth medium were used as control (Cntrl). For comparison of molecular composition of MV with other types of EV, EV from murine plasma (Plasma) and B16-F10 melanoma cell line (Mel) were used. (A) Silver stained gel showing protein loading for Western blot analyses and banding pattern of proteins from MV, 17IIA11 cells, and EV from plasma and melanoma cells. Asterisk indicates protein bands that are differentially expressed between MV from treated and untreated cells; pound sign indicates a protein equally expressed in MV from both treated and untreated cells. (B) Western blot analyses of proteins supporting mineralization: TNAP, PHOSPHO1, and annexin V (AnxV); exosomal markers: HSP70 and CD81; cytosolic and cell organelle proteins: α-tubulin, GAPDH, Rab5, GM130, Grp78, cytochrome C (CytoC), Lamp1, Lamp2a, histone 1 (H1), and histone 3a (H3a).

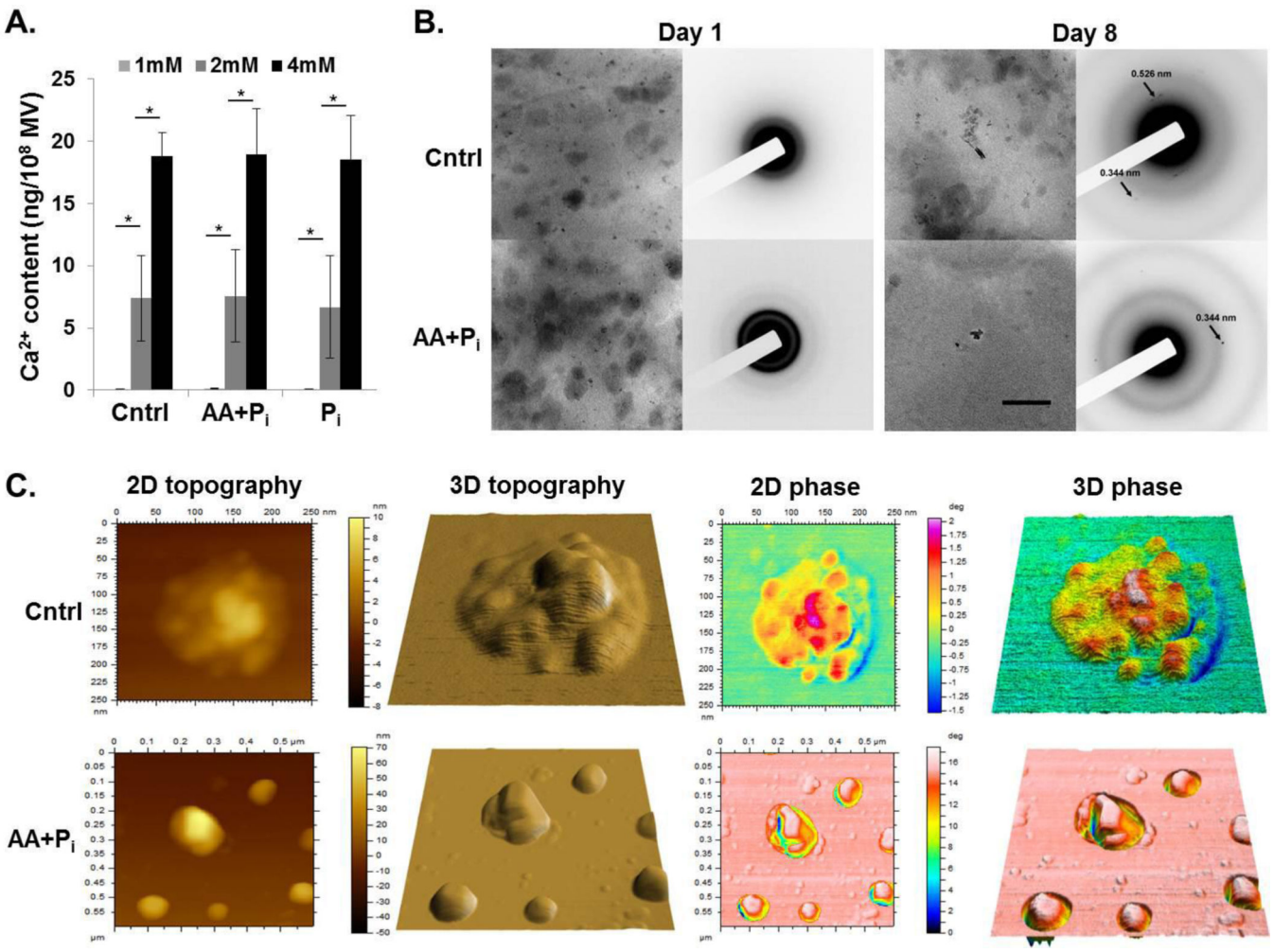

Figure 5. MV secreted by 17IIA11 cells are able to mineralize

(A) Bar graphs showing Ca^{2+} concentration-dependent accumulation of Ca^{2+} in MV isolated from 17IIA11 cells grown for 24h in standard growth medium (Cntrl), in osteogenic medium ($AA+P_i$), or in standard growth medium supplemented with 10mM P_i (P_i). Under conditions of 1 mM Ca^{2+} in the calcification buffer, there was no detectable Ca^{2+} in MV. (B) Bright field TEM micrographs (left columns) and corresponding electron diffraction patterns (right columns) of MV preparations collected from cells grown either in standard growth medium (Cntrl) or in osteogenic medium ($AA+P_i$) for 1 day and 8 days. All micrographs were acquired at the same magnification. The scale bar corresponds to 200 nm. (C) AFM images of MV collected from cells grown either in standard growth medium (Cntrl) or in osteogenic medium ($AA+P_i$) for 8 days. From left to right: 2D topography, 3D topography, 2D phase and 3D phase images. Scan size of the control sample: 600 nm × 600 nm. Scan size of the $AA+P_i$ sample: 250 nm × 250 nm.

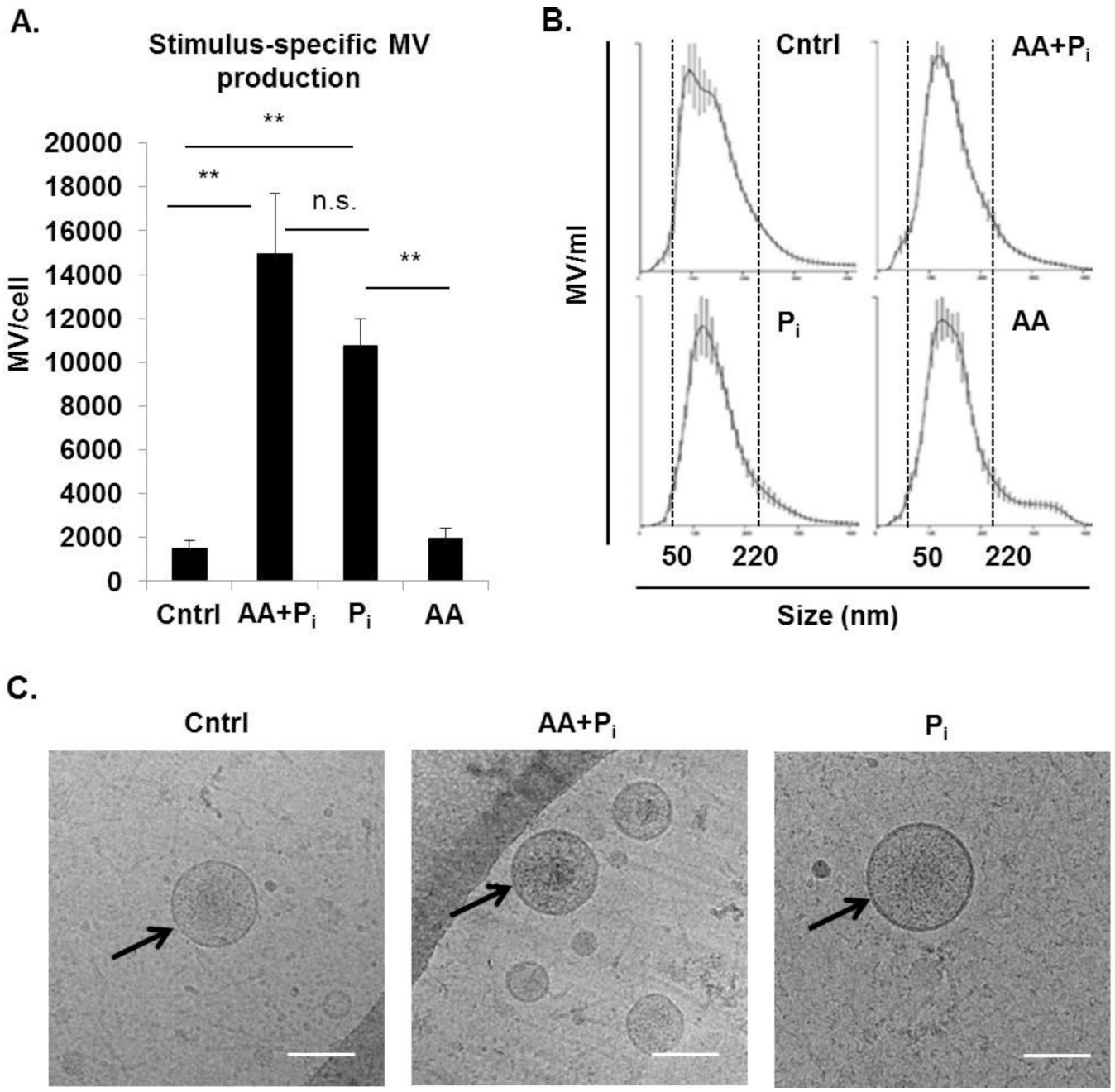

Figure 6. Inorganic phosphate (P_i) alone is sufficient to induce MV secretion from 17IIA11 cells

(A) Comparison of the number of MV released by cells within 24h of stimulation with standard osteogenic medium (ascorbic acid and P_i; AA + P_i), 10 mM Na-P_i buffer (P_i), or ascorbic acid (AA), with cells cultured in standard growth medium (Cntrl). Data are represented as the mean values of three independent experiments ± SD, *$p<0.05$ and **$p<0.005$. (B) Representative graphs showing MV size distribution in all culture conditions. Dotted lines indicate the size range of vesicles for each cell line. (C) Representative cryo-electron microscopy images of MV secreted by cells cultured for 24h in

standard growth medium (Control) or in standard osteogenic medium (AA+P_i), or in the presence of 10 mM Na-P_i buffer (P_i). Scale bar = 100nm.

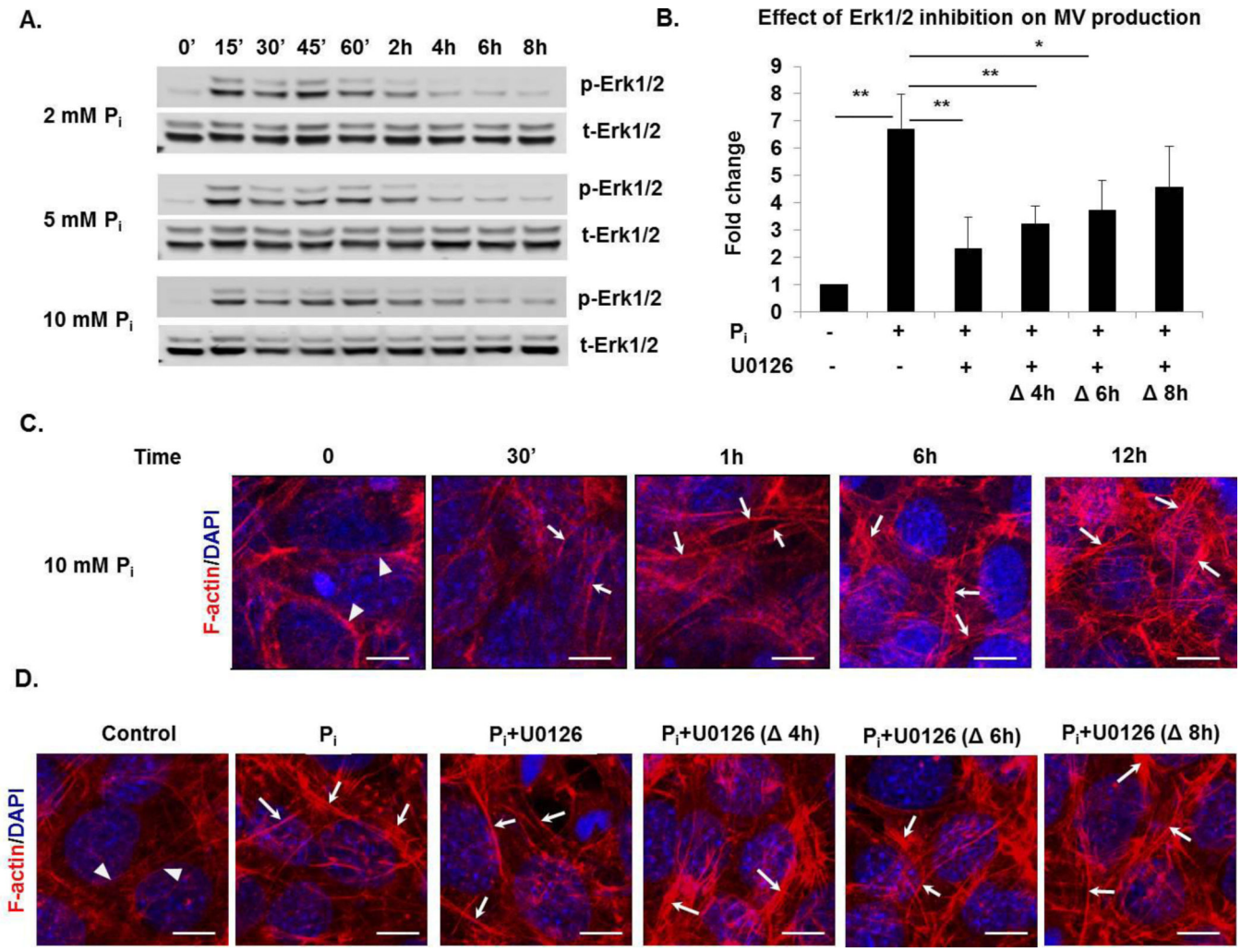

Figure 7. Phosphate-induced Erk1/2 activation mediates MV secretion from 17IIA11 cells

(A) Western blot analyses of total Erk1/2 (t-Erk1/2) and activated Erk1/2 (p-Erk1/2) in 17IIA11 cells treated with 2, 5, and 10 mM Na-P_i (P_i) for 0min, 15min, 30min, 45min, 1h, 2h, 4h, 6h, and 8h. (B) Comparison of MV secretion from 17IIA11 cells treated with 10 mM Na-P_i in the presence and absence of Erk1/2 inhibitor U0126 (10 μM). U0126 was added to growth medium either together with P_i (0h) or 4h, 6h, or 8h after P_i. MV were isolated 12h after P_i treatment and quantified using nanoparticle tracking analysis. Graphs depict fold changes in the number of MV secreted per cell in comparison to untreated cells. Data are represented as the mean values of three independent experiments ± SD, *$p<0.05$ and **$p<0.005$. (C) Representative microscopic images of filamentous actin (F-actin; red fluorescent staining) showing changes in F-actin organization induced by treatment of 17IIA11 cells with 10 mM Na-P_i. F-actin was analyzed at 30min, 1h, 6h, and 12h after P_i treatment. Blue DAPI staining: nuclei. (D) Representative images showing F-actin organization in 17IIA11 cells treated with 10 mM Na-P_i for 12h in the presence or absence of Erk1/2 inhibitor U0126 (10 μM). U0126 was added to growth medium either together with P_i (0h) or 4h, 6h, or 8h after P_i. Arrows indicate elongated and condensed F-actin fibers

in 17IIA11 cells treated with P_i, arrowheads indicate perinuclear localization of actin in untreated cells.